Computing Triangulations of Mapping Tori of Surface Homeomorphisms

Peter Brinkmann and Saul Schleimer

CONTENTS

We present the mathematical background of a software package that computes triangulations of mapping tori of surface homeomorphisms, suitable for Jeff Weeks's program SnapPea. The package is an extension of the software described in [Brinkmann 2000]. It consists of two programs. `jmt` computes triangulations and prints them in a human-readable format. `jsnap` converts this format into SnapPea's triangulation file format and may be of independent interest because it allows for quick and easy generation of input for SnapPea. As an application, we obtain a new solution to the restricted conjugacy problem in the mapping class group.

1. INTRODUCTION

An earlier paper [Brinkmann 2000] described a software package that provides an environment for computer experiments with automorphisms of surfaces with one puncture. The purpose of this paper is to present the mathematical background of an extension of this package that computes triangulations of mapping tori of such homeomorphisms, suitable for further analysis with SnapPea [Weeks 1993].

Pseudo-Anosov homeomorphisms are of particular interest because their mapping tori are hyperbolic 3-manifolds of finite volume [Thurston 1986a]. The software described in [Brinkmann 2000] recognizes pseudo-Anosov homeomorphisms. Combining this with the programs discussed here, we obtain a powerful tool for generating and analyzing large numbers of hyperbolic 3-manifolds.

The software package described in [Brinkmann 2000] takes an automorphism φ of a surface S with one puncture (given as a sequence of Dehn twists) and computes the induced outer automorphism of the fundamental group of S, represented by a homotopy equivalence $f\colon G \to G$ of a finite graph $G \subset S$ homotopy equivalent to S, together with a loop σ

This research was partially conducted by Brinkmann for the Clay Mathematics Institute.

2000 Mathematics Subject Classification: 57M27, 37E30.

Keywords: Mapping tori of surface automorphisms, pseudo-Anosov automorphisms, mapping class group, conjugacy problem.

in G homotopic to a loop around the puncture of S. The map f and the loop σ determine φ up to isotopy [Brinkmann 2000, Section 5.1].

In Section 2, we describe an effective algorithm for computing a triangulation of the mapping torus of $\varphi\colon S \to S$, given only $f\colon G \to G$ and σ (Theorem 2.3). We also present an analysis of the complexity of this algorithm (Proposition 2.4). The first part of the software package is a program (called `jmt`) that implements this procedure. The program `jmt` prints its output in an intermediate human-readable format.

In Section 3, we explain how to use the software discussed here and the isometry checker of SnapPea to solve the restricted conjugacy problem in the mapping class group (i.e., the question of whether two pseudo-Anosov homeomorphisms are conjugate in the mapping class group). This problem was previously solved in [Mosher 1986] and [Hemion 1979]. One distinguishing feature of our solution is that much of it has already been implemented.

Section 4 presents sample computations that exhibit some of the capabilities of the combination of SnapPea and the software discussed here.

The Appendix discusses the second program in the software package (called `jsnap`), which converts the intermediate format of `jmt` into SnapPea's triangulation file format. Since SnapPea's format is rather complicated, it is not easy to generate input files for SnapPea, and `jsnap` may be of independent interest because it allows users to generate input for SnapPea without having to understand SnapPea's file format.

Immediate applications of the software described here include an experimental investigation of possible relationships between dynamical properties of pseudo-Anosov homeomorphisms (as computed by the first author's train track software) and topological properties of their mapping tori (as computed by SnapPea). For example, one might look for a relationship between growth rate and volume. Another area where the package described in this paper has already been used is the study of slalom knots as introduced by Norbert A'Campo [1998].

The software is written in Java and should be universally portable. The programs `jmt` and `jsnap` are command line software and can be used to examine a large number of examples as a batch job. A graphical user interface with an online help feature is also available.

2. COMPUTING TRIANGULATIONS

Let $\varphi\colon S \to S$ be an automorphism of a surface S with one puncture, represented by a homotopy equivalence $f\colon G \to G$ of a finite graph G and a loop σ in G representing a loop around the puncture of S (see Section 1). There is no loss in assuming that $f\colon G \to G$ maps vertices to vertices and that the restriction of f to the interior of each edge of G is an immersion.

In this section, we outline an effective procedure that computes a triangulation of the mapping torus of φ given only f and σ. To this end, we construct a simplicial 2-complex K and a face pairing e with the following properties.

1. The space $|K|$ is homeomorphic to a torus.
2. For each 2-simplex Δ of K, there exists a 2-simplex Δ' of K and an orientation reversing simplicial homeomorphism $e_\Delta\colon \Delta \to \Delta'$ such that $e_{\Delta'}^{-1} = e_\Delta$.
3. The space K/e is homotopy equivalent to the mapping torus of f.
4. If we let $M = (\text{cone over } K)/e$ and obtain M' from M by removing the cone point, then M' is a 3-manifold (in particular, the links of vertices in M' are 2-spheres).

In this situation, M' is homotopy equivalent to the mapping torus of f, and this in turn is homotopy equivalent to the mapping torus M_φ of φ. As M' is a 3-manifold, M' is homeomorphic to M_φ [Johannson 1979, p. 6].

The triangulation of K induces a triangulation of M, i.e., the tetrahedra of M are cones over the triangles of K. The vertices of K give rise to finite vertices of M, and the cone point is an ideal vertex corresponding to the torus cusp of M_φ. By computing the links of vertices, SnapPea recognizes finite vertices (whose links are 2-spheres) and ideal vertices (whose links are tori or Klein bottles).

Hence, we have reduced the problem of constructing a triangulation of the mapping torus of φ to the construction of the 2-complex K and face pairing e, given only the homotopy equivalence $f : G \to G$

and the loop σ. The construction of K and e is the purpose of the remainder of this section.

The construction of K and e proceeds in two steps. We construct the 2-torus T by gluing annuli using Stallings's folding construction [1983]. Then we construct a triangulation and a face pairing for each of the annuli.

Step 1: Subdividing and Folding

We review the notion of subdividing and folding [Stallings 1983; Bestvina and Handel 1992]. Let G, G' be finite graphs, and let $f\colon G' \to G$ be a map that maps vertices to vertices and edges to edge paths.

If f fails to be an immersion, then there exist two distinct edges a, b in G' emanating from the same vertex such that $f(a)$ and $f(b)$ have a nontrivial initial path in common. We construct a new graph G'_1 by subdividing a into two edges a_1, a_2 and subdividing b into b_1, b_2.

Now f factors through G'_1, i.e., there are maps $s\colon G' \to G'_1$ and $g\colon G'_1 \to G$ such that $f = g \circ s$. Moreover, we can choose s and g such that $s(a) = a_1a_2$, $s(b) = b_1b_2$ and $g(a_1) = g(b_1)$. We obtain a new graph G'_2 from G'_1 by identifying the edges a_1 and b_1. Then g factors through G'_2, i.e., there is a map $h\colon G'_2 \to G$ such that $g = h \circ p$, where p is the natural projection $p\colon G'_1 \to G'_2$ (see Figure 1). We refer to this process as *folding* a_1 and b_1.

Remark 2.1. The notion of folds used in [Bestvina and Handel 1992] differs slightly from that introduced in [Stallings 1983]. Bestvina and Handle consider homotopy equivalences $f : G \to G$, and folding changes *both* the domain and the range of f, whereas Stallings considers maps $f : G' \to G$, and folding only affects the domain G'. The notion of folds used in this paper is a slight modification of the folds in [Stallings 1983].

The remainder of this subsection details how to construct a sequence of graphs and maps

$$G = G_0 \xrightarrow{s_0} G_1 \xrightarrow{p_0} G_2 \ldots G_{2n-2} \xrightarrow{s_{n-1}} G_{2n-1} \xrightarrow{p_{n-1}} G_{2n} \xrightarrow{g_n} G$$

such that

$$f = g_n \circ p_{n-1} \circ s_{n-1} \circ \ldots \circ p_0 \circ s_0,$$

where $s_i\colon G_{2i} \to G_{2i+1}$ is a subdivision, $p_i\colon G_{2i+1} \to G_{2i+2}$ is a Stallings fold, and $g_n\colon G_{2n} \to G_0$ is an immersion. Since f is a homotopy equivalence, g_n will be onto, hence a homeomorphism. Moreover, for each $i = 0, \ldots, 2n$, we will construct a loop σ_i in G_i corresponding to a loop around the puncture of S.

Let $f\colon G \to G$ be induced by a homeomorphism $\varphi\colon S \to S$, and let σ denote an edge loop in G corresponding to a loop around the puncture of S. Let $G = G_0$, $g_0 = f\colon G_0 \to G$, and $\sigma_0 = \sigma$.

Suppose that g_0 is not an immersion. Then there exist two edges a, b emanating from the same vertex in G_0 such that $g_0(a)$ and $g_0(b)$ have a common initial segment. Since g_0 is induced by the homeomorphism $\varphi\colon S \to S$, we can find a and b such that a and b are adjacent in the embedding of G_0 in S.

Since the loop σ_0 in G is homotopic to a loop around the puncture, a and b will be adjacent in the spelling of σ_0. Hence, we can detect a and b algorithmically by looking for cancellation between the images of adjacent edges in the spelling of σ_0.

We obtain G_1 from G_0 by subdividing a and b, and we obtain G_2 from G_1 by folding the initial segments of a and b. As above, we construct maps $s_0\colon G_0 \to G_1$, $p_0\colon G_1 \to G_2$, and $g_1\colon G_2 \to G$ such that $g_0 = g_1 \circ p_0 \circ s_0$. Let $\sigma_1 = s_0(\sigma_0)$ and obtain σ_2 from $p_0(\sigma_1)$ by tightening. Since the edges a and b are adjacent in the embedding of G in S, the embedding of G_0 in S induces an embedding of G_1 and G_2 in S, and σ_1 and σ_2 are homotopic to σ_0 in S.

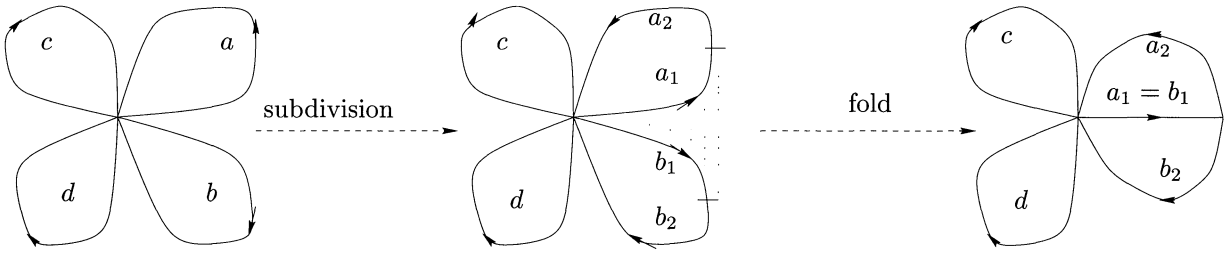

FIGURE 1. Subdividing and folding.

Note that the *size* of g_1, i.e., the sum of the lengths of the images under g_1 of the edges in G_2, is strictly smaller than the size of g_0. Hence, after repeating this construction finitely many times, we reach a map $g_n\colon G_{2n} \to G$ that cannot be folded and thus has to be an immersion. We have found the desired sequence of subdivisions and folds.

Example 2.2. Let G be the graph with one vertex and four edges, labeled $a, \ldots, d$, embedded in a punctured surface S of genus 2 as shown in Figure 2.

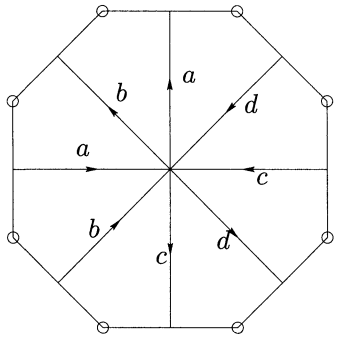

FIGURE 2. The graph G embedded in the surface S. The corners of the octagon correspond to the puncture of S. Two faces of the octagon are glued via an orientation-reversing map if the edge labels match up.

We consider the following homotopy equivalence $f\colon G \to G$, induced by an automorphism of S:

$$f(a) = a\underline{cd\bar{c}\bar{b}} \qquad f(b) = bcd\bar{c}b\underline{cd\bar{c}\bar{b}}$$
$$f(c) = bcd\bar{d} \qquad f(d) = dd\bar{c}bd$$
$$\sigma = a\bar{b}\bar{a}bcd\bar{c}d$$

In $f(\sigma)$, cancellation occurs between the underlined parts of $f(a)$ and $f(\bar{b})$, and we subdivide a and b in preparation for folding, which gives us the maps $s_0\colon G \to G_1$ and $g_1\colon G_1 \to G$ (see Figure 1). In order to reduce notational complexity, we only change the labels of those edges that are subdivided.

$$s_0(a) = a_1a_2 \qquad s_0(b) = b_1b_2$$
$$s_0(c) = c \qquad s_0(d) = d$$
$$\sigma_1 = a_1a_2\bar{b}_2\bar{b}_1\bar{a}_2\bar{a}_1b_1b_2cd\bar{c}d$$

Now we fold the edges $\bar{a_2}$ and $\bar{b_2}$.

$$p_0(a_1) = a_1 \qquad p_0(a_2) = b_2$$
$$p_0(b_1) = b_1 \qquad p_0(b_2) = b_2$$
$$p_0(c) = c \qquad p_0(d) = d$$

Finally, we compute the map $g_1\colon G_2 \to G$.

$$g_1(a_1) = a \qquad g_1(b_1) = bcd\bar{c}b$$
$$g_1(b_2) = cd\bar{c}\bar{b} \qquad g_1(c) = bcd\bar{d}$$
$$g_1(d) = dd\bar{c}bd \qquad \sigma_2 = a_1\bar{b}_1\bar{b}_2\bar{a}_1b_1b_2cd\bar{c}d$$

Step 2: Triangulating Annuli

We can interpret the loops σ_i as immersions

$$\sigma_i\colon S^1 \to G_i.$$

The preimage of the vertex set of G_i subdivides S^1 into intervals, and the restriction of σ_i to such an interval is a homeomorphism onto the interior of an edge in G_i. Hence, we can label each interval with the corresponding edge in G_i. We refer to this construction as *spelling* σ_i *along* S^1.

Now, for each $i \in \{0, \ldots, 2n\}$, we take an annulus A_i and spell the word σ_i along one boundary component and σ_{i+1} along the other. We orient the two boundary components of A_i such that they are freely homotopic as oriented loops.

This labeling defines a gluing of A_i and A_{i+1}, and the homeomorphism $g_n\colon G_{2n} \to G = G_0$ induces a gluing of A_{2n-1} and A_0 (which we refer to as the *final gluing*), giving us the desired torus T (Figure 3). Figure 4 shows the gluing of A_0 and A_1 for Example 2.2.

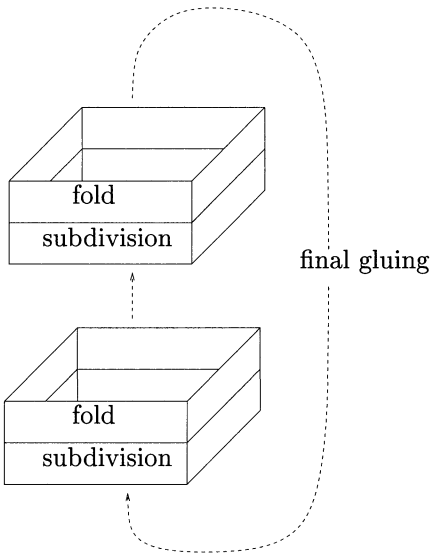

FIGURE 3. Decomposition into annuli.

Fix some $i \in \{0, \ldots, 2n\}$ and spell σ_i along S^1. Notice that each label on S^1 occurs twice, once for each direction (see Example 2.2 and Figure 2). If

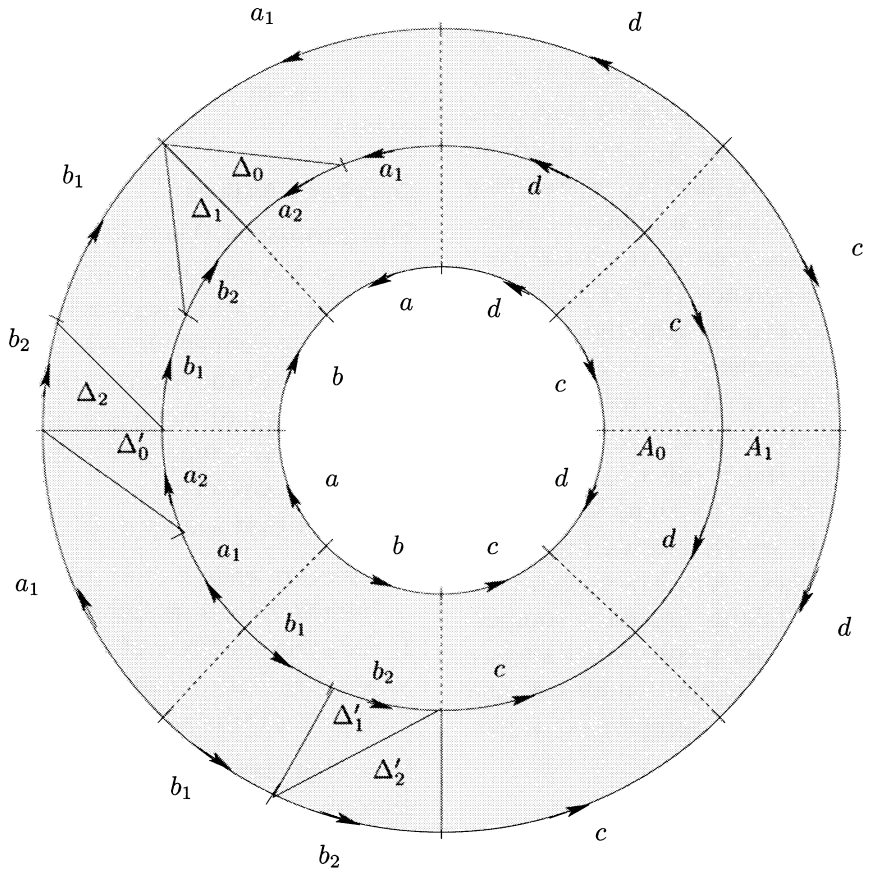

FIGURE 4. The gluing of A_0 and A_1 for Example 2.2.

we identify corresponding intervals, we obtain the graph G_i, and if we take the cone over S^1, remove the cone point, and identify intervals with identical labels, then we obtain the surface S [Brinkmann 2000, Section 5.1].

Hence, we only need to extend the edge pairing on the boundary of the annulus A_i to an appropriate face pairing of a triangulation of all of A_i. Recall that we want to choose the face pairing in such a way that the cone over T (with the cone point removed) becomes a 3-manifold when we identify corresponding triangles.

We first find a suitable triangulation of an annulus A_{2i} corresponding to a subdivision s_i. We decompose A_{2i} into rectangles corresponding to edges that are not subdivided and pentagons corresponding to those edges that are subdivided (see Figure 4). The edge pairing on the boundary of A_{2i} induces a pairing of rectangles (or pentagons as the case may be). Finding a triangulation of A_{2i} that is compatible with this pairing is straightforward.

We now construct a suitable triangulation of an annulus A_{2i+1} corresponding to a fold p_i. Edges that are not involved in the fold give rise to paired rectangles contained in A_{2i+1} (see Figure 4), and as above, we easily find a triangulation of these rectangles that is compatible with the pairing.

Let a, b denote the two edges involved in the fold, i.e., we have $p_i(a) = p_i(b) = b'$. By exchanging a and b or reversing the orientation of a and b as necessary, we may assume that the loop σ_{2i+1} has a subpath of the form $w = a\bar{b}u\bar{a}$ or $w = a\bar{b}ub$, where u is a path that contains neither a nor b. For concreteness, we focus on the case $w = a\bar{b}u\bar{a}$. The first fold of Example 2.2 falls into this case, with $w = a_2\bar{b}_2\bar{b}_1\bar{a}_2$. The construction in the remaining case is similar.

The loop σ_{2i+2} has a corresponding subpath of the form $w' = u'\bar{b}'$. Let Δ_0 be the triangle spanned by the initial endpoint of w' and the occurrence of a in w. We pair Δ_0 with the triangle Δ_0' spanned by the terminal endpoint of w' and the occurrence of $\bar{a}$ in w (see Figure 4).

Let Δ_1 be the triangle spanned by the occurrence of $\bar{b}$ in w and the initial endpoint of w', and let Δ_2 be the triangle spanned by the occurrence of $\bar{b}'$ in w' and the terminal endpoint of u. Observe that after identifying paired edges, Δ_1 and Δ_2 have a side in common, so we can think of Δ_1 and Δ_2 as spanning a rectangle between $\bar{b}$ and $\bar{b}'$, which induces a triangulation of the rectangle spanned by the occurrence of b in σ_{2i+1} and the occurrence of $\bar{b}$ in σ_{2i+2} (see Figure 4). This completes the triangulation and face pairing of A_{2i+1}, which completes our construction.

Given the triangulation of A_{2i+1} we have constructed above, we can think of the annulus A_{2i+1} as interpolating between the graph G_{2i+1} and the graph G_{2i+2}. In other words, we think of the fold as occurring continuously, by identifying larger and larger segments of the edges a and b (see Figure 5). Moreover, this continuous folding process is compatible with the embedding of the graphs in the surface S. This observation shows that the complex K and its triangulation have the desired properties, in particular Property 4.

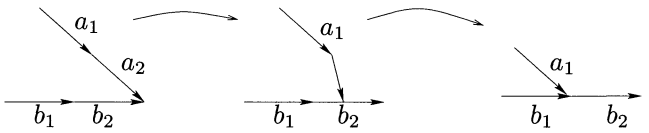

FIGURE 5. Continuous fold for Example 2.2.

Summing up, we have obtained the main result of this paper:

Theorem 2.3. *Let f be a homotopy equivalence of a finite graph G, representing a homeomorphism φ of a once-punctured surface. Then the following is an effective procedure for computing a triangulation of the mapping torus of φ.*

1. *Decompose the homotopy equivalence $f\colon G \to G$ into a sequence of subdivisions and folds, followed by a homeomorphism (Step 1 in* Section 2).
2. *Obtain the torus K as a gluing of one annulus for each subdivision and fold in the above decomposition* (Figure 3).
3. *Triangulate the individual annuli and construct a face pairing (Step 2 in* Section 2).
4. *Construct a triangulation of the mapping torus of the surface homeomorphism φ by taking the cone of K and glue tetrahedra according to the face pairing.* □

The program `jmt` is an implementation of this procedure.

Complexity Analysis

The purpose of this subsection is to obtain an estimate on the number of tetrahedra in the triangulation that we have constructed.

We have defined the size of a map $h\colon G' \to G$ to be the sum of the lengths (in the usual path metric) of the images of the edges of G'. For example, the size of the first map in Example 2.2 is 23. Let $S(h)$ denote the size of h.

We say that a map $g\colon G' \to G$ is *tight* if

1. for every edge e of G', the restriction of g to the interior of e is an immersion, and
2. for every vertex v of G', there are two edges emanating from v that cannot be folded (not even after a subdivision).

Note that tightness can always be achieved by homotopy.

Proposition 2.4. *Let $f : G \to G$ be a tight homotopy equivalence representing a homeomorphism φ of a once-punctured surface of genus g, and assume that G has no vertices of valence less than three. Then the number of tetrahedra in the triangulation of M_φ is bounded by $16(5g-2)S(f)$.*

Proof. Since folding reduces size and annuli come in pairs (a subdivision annulus followed by a folding annulus), the number of annuli is bounded above by $2S(f)$. A simple application of Euler characteristics shows that G has no more than $6g-3$ edges because the valence of each vertex is at least three. Subdividing and folding, however, may create additional edges as well as vertices of valence one or two, so we need to understand the effect of subdividing and folding on the number of edges.

To this end, we introduce the notion of *partial folds*, i.e., folds where both participating edges have to be subdivided, and *full folds*, i.e., folds where at least one of the participating edges is not subdivided [Bestvina and Handel 1992]. Clearly, a subdivision followed by a full fold does not increase the number of edges, whereas a subdivision followed by a partial fold increases the number of edges by one.

A partial fold reduces the number of possible folds by one because the map resulting from it is an immersion around the new vertex created by the fold, so the only folds that are possible after a partial fold are those that were available before.

Similarly, a full fold does not increase the number of possible folds. This means that the number of partial folds that occurs in our construction is bounded by the number of folds that the map $f\colon G \to G$ admits. Since f is tight, the number of folds at one vertex v is bounded by $\mathrm{val}(v) - 2$. Summing up, we see that the number of possible folds is bounded by

$$\sum_{v \in G^{(0)}} (\mathrm{val}(v) - 2) = -2\chi(G) = 4g - 2.$$

Hence, the number of edges after a fold is bounded by $6g - 3 + 4g - 2 = 10g - 5$. Subdivisions increase the number of edges, so the number of edges at any point in our construction is bounded by $10g - 4$.

The number of tetrahedra belonging to one annulus is bounded above by $8(5g - 2)$ (four tetrahedra per edge), which gives us a theoretical upper bound of $16(5g - 2)S(f)$ on the number of tetrahedra in our triangulation of M_φ. □

Similar arguments show that for fixed genus, the time it takes to compute a triangulation is linear in the size of the input. We note that in practice, partial folds seldom occur, and triangulations tend to be considerably smaller than the bound given in Proposition 2.4.

3. SOLVING THE CONJUGACY PROBLEM

The algorithm from Section 2 and SnapPea's isometry checker provide a practical way of testing a necessary condition for two pseudo-Anosov homeomorphisms φ, γ to be conjugate in the mapping class group. Namely, we can compute the mapping tori of φ and γ as in Section 2, and then SnapPea's isometry checker will determine whether the two mapping tori are isometric. If they are not isometric, we can immediately conclude that the φ and γ are not conjugate. However, if the mapping tori are isometric, we cannot yet conclude that they are conjugate. The purpose of this section is to provide an effective sufficient criterion for conjugacy.

Problem 3.1. Let γ and φ be automorphisms of a surface S with one puncture. Both automorphisms are assumed to be presented as products of Dehn twists on S.

The *conjugacy problem* asks for a decision procedure to determine whether or not γ and φ are conjugate in the mapping class group of S. That is, does there exist an automorphism, φ, of S such that $\gamma = \varphi^{-1}\varphi\varphi$?

The *restricted conjugacy problem* is slightly easier in that it assumes that γ and φ are in fact pseudo-Anosov. As the software described in [Brinkmann 2000] can decide whether or not a mapping class element is pseudo-Anosov we will, from now on, only consider this simpler problem.

A complete (albeit impractical) solution for the conjugacy problem has been given by Hemion [1979]. The restricted case has also been solved by Mosher [1986].

Notation

In order to describe our solution of the restricted conjugacy problem, we need to introduce some notation. Let $\gamma\colon S \to S$ and $\varphi\colon S \to S$ be pseudo-Anosov homeomorphisms with isometric mapping tori. SnapPea will detect this and compute an isometry $h\colon M_\gamma \to M_\varphi$.

Let $i_\gamma\colon S \to M_\gamma$ and i_φ be the two inclusion maps that realize S as a fiber of the induced fiber structures $\mathcal{F}_\gamma$ and $\mathcal{F}_\varphi$ on M_γ and M_φ. Set $F_\gamma = i_\gamma(S)$ and define F_φ in a similar fashion.

Let $p_\gamma\colon M_\gamma \to S^1$ be the map from M_γ to the circle induced by $\mathcal{F}_\gamma$ and define p_φ similarly.

Let $\sigma \in \mathrm{Mod}(M_\varphi)$ denote a typical element of the isometry group of M_φ. As M_φ is hyperbolic, $\mathrm{Mod}(M_\varphi)$ is a finite group and can be computed by SnapPea. Set $G_\sigma = \sigma h(F_\gamma)$.

Finally, pick any $g \in \pi_1(M_\gamma)$ with the property that $(p_\gamma)_* g = 1 \in \mathbb{Z}$. We say that such a loop *represents the S^1-orientation.* If $(p_\varphi \sigma h)_* g$ equals 1 we say that σh *preserves S^1-orientation*; otherwise that it reverses orientation.

Retriangulation and the Fundamental Group

Before solving the restricted conjugacy problem we'll need a pair of subroutines to determine the images of elements of $\pi_1(M_\gamma)$ under the map $(p_\varphi \sigma h)_*$.

First, we need an algorithm to decide whether $(p_\varphi)_*$: $\pi_1(G_\sigma) \to \mathbb{Z}$ has trivial image. The idea here is to keep track of a set of generators for $\pi_1(S)$ under the maps i_γ, h, σ and p_φ. Unfortunately, these homeomorphisms do not all respect common simplicial structures on M_γ and M_φ. To fix this problem one must find an appropriate set of generators in each retriangulation of M_γ. Then, once SnapPea finds a geometric triangulation of M_γ, we can push the generators onto the one-skeleton of the Ford domain. The isometry σh takes them to edge paths in the one-skeleton of M_φ where we can reverse the process. Finally, p_φ projects the generators of $\pi_1(G_\sigma)$ to the circle where it is easy to check whether or not they are all contractible.

Second, we will need an algorithm which decides whether σh preserves S^1-orientation. To do this, construct any loop $g \in \pi_1(M_\gamma)$ which represents the S^1-orientation. As in the previous algorithm take the image of g under the map $(p_\varphi \sigma h)_*$. Check that this image is the positive generator of $\pi_1(S^1)$.

The bookkeeping problem of keeping track of surface subgroups of $\pi_1(M^3)$ under retriangulation does not yet have an implemented solution. We would be very interested in the work of any reader who is willing to write such a program. It should be remarked that the subroutines above do a little more work than is strictly necessary. It would suffice to keep track of a two-chain representing the fiber of M_γ. This is another straightforward problem that, as far as we know, does not yet have an implemented solution.

The Algorithm

Given two pseudo-Anosov homeomorphisms

$$\gamma, \varphi\colon S \to S,$$

construct the mapping tori, M_γ and M_φ. If SnapPea reports that M_γ and M_φ are not isometric, we conclude that γ cannot be conjugate to φ. This resolves the issue for a vast majority of possible pairs of γ and φ.

Now, suppose SnapPea reports the two mapping tori are isometric. We cannot yet conclude that the two automorphisms are conjugate. It may be that γ and φ have homeomorphic mapping tori but are not conjugate because they give rise to distinct fiber structures in the resulting three manifold. Also, it may happen that γ and φ induce identical fiber structures while reversing S^1-orientation. In this case it is possible to show that γ is conjugate to φ^{-1}.

If $\pi_1(G_\sigma)$ has nontrivial image under $(p_\varphi)_*$ then clearly G_σ is not isotopic to F_φ. We conclude that if $\pi_1(G_\sigma)$ has nontrivial image in $\pi_1(S^1) = \mathbb{Z}$ for every σ in $\mathrm{Mod}(M_\varphi)$ then γ is not conjugate to φ.

We claim that if there exists some σ such that σh preserves S^1-orientation and $\pi_1(G_\sigma)$ is contained in the kernel of the natural projection, then γ is conjugate to φ, which completes our solution of the restricted conjugacy problem. The rest of this section is devoted to a proof of this claim.

Isotoping G_σ

Assume now that $\pi_1(G_\sigma)$ has trivial image in $(p_\varphi)_*$ for some fixed $\sigma \in \mathrm{Mod}(M_\varphi)$. At this point we need a weak form of Theorem 4 from [Thurston 1986b]:

Theorem 3.2. *G_σ is properly isotopic to an embedded surface that is either a leaf of $\mathcal{F}_\varphi$, or has only saddle singularities for the induced singular foliation of G_σ. The boundary component of the isotoped G_σ is either a leaf of $\mathcal{F}_\varphi|\partial M_\varphi$ or is transverse to $\mathcal{F}_\varphi|\partial M_\varphi$.* □

We use this as follows:

Corollary 3.3. *If $\pi_1(G_\sigma)$ is in the kernel of $(p_\varphi)_*$ then G_σ is isotopic to F_φ.*

Proof. Suppose, to obtain a contradiction, that G_σ is not isotopic to F_φ. By Thurston's theorem we may isotope G_σ so that the induced foliation has only saddle singularities.

Let $M_\mathbb{Z} = F_\varphi \times \mathbb{R}$ be the infinite cyclic cover of M coming from $\mathcal{F}_\varphi$. By assumption we may lift G_σ to $M_\mathbb{Z}$. Note that projection onto the second factor $M_\mathbb{Z} \to \mathbb{R}$ gives a Morse function when restricted to G_σ. However this Morse function must have a maximum. The induced foliation of G_σ has a singularity at this maximum, but this singularity cannot possibly be a saddle singularity. This is a contradiction. □

Thus we may isotope σh so as to obtain $G_\sigma = F_\varphi$. Cutting along F_γ and F_φ we obtain a map h': $S \times I \to S \times I$ that takes $S \times 0$ and $S \times 1$ to $S \times 0$ and $S \times 1$, but not necessarily in that order. It may be that σh reverses the S^1-orientation.

It follows that h', and hence σh, is isotopic to a map that preserves fibers. (See, for example, [Waldhausen 1968, Lemma 3.5].) Letting $h_0 = (\sigma h)|F_\gamma$ we find that either $\gamma = h_0^{-1}\varphi h_0$ or $\gamma = h_0^{-1}\varphi^{-1}h_0$ depending on whether σh preserves or reverses S^1-orientation. This completes the proof of the claim and thus shows the correctness of our algorithm, which we sum up in the following theorem.

Theorem 3.4. *Let γ and φ be pseudo-Anosov homeomorphisms of a once punctured surface, S. The following is a procedure to decide whether the two mappings are conjugate in the mapping class group of S, if SnapPea is allowed as a subroutine.*

1. *Apply Theorem 2.3 to obtain the mapping tori, M_γ and M_φ.*
2. *Using `jsnap` and SnapPea, determine whether or not M_γ and M_φ are isometric. If not, then γ is not conjugate to φ.*
3. *Using SnapPea, enumerate all isometries between M_γ and M_φ.*
4. *Determine whether any of these isometries are S^1-orientation and fiber preserving. If none are, then γ is not conjugate to φ. Otherwise, γ is conjugate to φ.* □

The complexity of this algorithm depends on the complexity of SnapPea, which we treat as a black box in this paper.

4. SAMPLE COMPUTATIONS

We present some sample computations illustrating the power of the software discussed here. We define surface automorphisms as compositions of Dehn twists with respect to the set of curves of Figure 6. We equip the surface with a normal vector field. When twisting with respect to a curve c, we turn right whenever we hit c (and left for inverse twists). The set of these Dehn twists generates the mapping class group [Lickorish 1964].

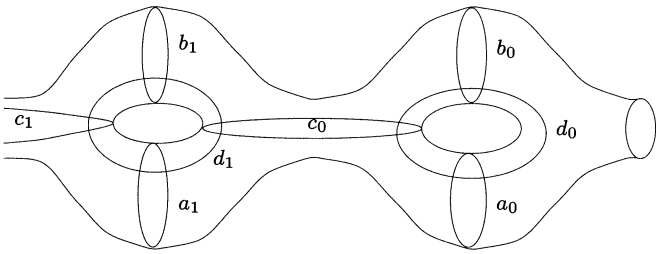

FIGURE 6. A set of generators of the mapping class group.

We first present an example for which we can easily verify correctness.

Example 4.1 (Figure-eight knot). An ideal triangulation of the complement of the figure-eight knot knot can be expressed as a gluing of two tetrahedra [Thurston 1997, pp. 39–42, 128–129]; see Figure 7.

According to SnapPea (see the Appendix for the input used), the fundamental group of the resulting manifold M has the presentation

$$\pi_1(M) \cong \langle x, y \mid \bar{y}\bar{x}\bar{x}\bar{x}\bar{y}xyyx = 1 \rangle. \qquad (4\text{–}1)$$

We modify this presentation by a sequence of Tietze transformations [Lyndon and Schupp 1977, II.2], obtaining

$$\begin{aligned}\pi_1(M) &\cong \langle x, y, z \mid \bar{y}\bar{x}\bar{x}\bar{x}\bar{y}xyyx = 1,\ y = z\bar{x} \rangle \\ &\cong \langle x, z \mid x\bar{z}\bar{x}\bar{x}\bar{z}xz\bar{x}z = 1 \rangle \\ &\cong \langle x, z \mid \bar{x}zx\bar{z}\bar{x}\bar{x}\bar{z}xz = 1 \rangle.\end{aligned}$$

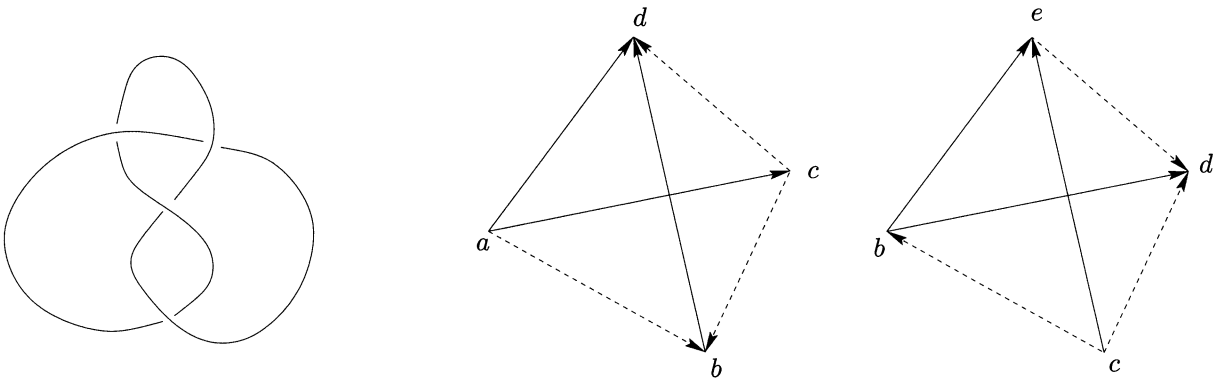

FIGURE 7. The complement of the figure-eight knot (left) can be expressed as a gluing of two ideal tetrahedra. Triangles are glued such that the line style and the direction of arrows are matched.

The last of these is the presentation of the fundamental group of the complement of the figure-eight knot given in [Burde and Zieschang 1985, Example 3.8].

Now let S be a punctured torus, and let $\varphi\colon S \to S$ be given by

$$\varphi = D_{a_0}^{-1} D_{d_0}.$$

The complement of the figure-eight knot is homeomorphic to the mapping torus of φ (we will verify this soon). Given this composition of Dehn twists, the train track software of [Brinkmann 2000] determines that φ is pseudo-Anosov with growth rate $\lambda \approx 2.61803399$, and SnapPea determines that the mapping torus M_φ is a hyperbolic 3-manifold of volume $V \approx 2.02988321$ with one torus cusp.

Moreover, the train track software computes the following topological representative $f\colon G \to G$ of φ, where G is a graph with one vertex and two edges.

$$\begin{aligned} f(a) &= ba \\ f(b) &= bba \\ \sigma &= a\bar{b}\bar{a}b \end{aligned}$$

This yields the following presentation of the fundamental group of the mapping torus M_φ of φ:

$$\pi_1(M_\varphi) \cong \langle a, b, t \mid \bar{t}at = ba,\ \bar{t}bt = bba \rangle.$$

A few Tietze transformations show that $\pi_1(M_\varphi)$ is the fundamental group of the figure-eight knot complement:

$$\begin{aligned} \pi_1(M_\varphi) &\cong \langle a, b, t \mid \bar{t}at = ba,\ \bar{t}bt = bba \rangle \\ &\cong \langle a, t \mid t\bar{a}\bar{a}ta\bar{t}\bar{a}\bar{t}a = 1 \rangle \\ &\cong \langle a, c \mid \bar{a}ca\bar{c}\bar{a}\bar{a}\bar{c}ac = 1 \rangle. \end{aligned}$$

As before, we have obtained the presentation given in [Burde and Zieschang 1985, Example 3.8].

Finally, the presentation of $\pi_1(M_\varphi)$ computed by SnapPea is

$$\pi_1(M_\varphi) \cong \langle x, y \mid \bar{x}\bar{y}\bar{y}\bar{y}\bar{x}yxxy = 1 \rangle,$$

agreeing with Presentation (4–1).

Alternatively, we can run the isometry checker of SnapPea on the two objects in order to see that we get the same hyperbolic 3-manifold in both cases.

Example 4.2 (Genus 3). Let S be a surface of genus 3 with one puncture, and let $\varphi\colon S \to S$ be given by

$$\varphi = D_{d_0} D_{c_0} D_{d_1} D_{c_1} D_{d_2} D_{a_2}^{-1}.$$

The train track software identifies φ as a pseudo-Anosov homeomorphism with growth rate

$$\lambda \approx 2.04249053,$$

and SnapPea finds that the mapping torus M_φ is a hyperbolic 3-manifold of volume $V \approx 4.93524268$ with one torus cusp.

These applications only show a small part of all the possibilities. The train track software computes a plethora of information about surface homeomorphisms [Brinkmann 2000], and SnapPea allows for a detailed analysis of (hyperbolic) 3-manifolds. We believe that the combination of the two packages may become a valuable tool for topologists.

APPENDIX: GENERATING INPUT FOR SNAPPEA

In order to generate input for SnapPea, the output of `jmt` has to be translated into SnapPea's triangulation file format by a second program (called `jsnap`). The purpose of this section is to discuss the intermediate format, which allows for quick and easy generation of input for SnapPea.

The intermediate format admits two types of input lines, for tetrahedra and for gluings. An input line defining a tetrahedron has the form

$$\texttt{T}\ \ v_1\ \ v_2\ \ v_3\ \ v_4,$$

where $v_1, \ldots, v_4$ are distinct labels of the vertices. Tetrahedra are glued implicitly if they have three vertices in common, and they can be glued explicitly by entering a line of the form

$$\texttt{G}\ \ v_1\ \ v_2\ \ v_3\ \ w_1\ \ w_2\ \ w_3,$$

where v_1, v_2, v_3 and w_1, w_2, w_3 are the labels of two faces of tetrahedra. In this gluing, the side $[v_1, v_2]$ is glued to the side $[w_1, w_2]$, the side $[v_2, v_3]$ is glued to the side $[w_2, w_3]$, etc. Empty lines and comments beginning with // are also allowed.

Although the four vertex labels of a tetrahedron have to be distinct, two or more vertices of a tetrahedron may be identified after gluing. Distinct vertex labels are only needed in order to uniquely specify the sides of tetrahedra.

While SnapPea's format is an extremely efficient representation of triangulations, understanding it requires some effort. The program `jsnap` acts as an interface between SnapPea and the human user.

If you can draw or visualize a triangulation of a 3-manifold, then you can also enter it into `jsnap`.

As an illustration, the gluing of Figure 7 is encoded as follows:

```
T a b c d
T b c d e
G b e d a c d
G c b e a b d
G c e d a c b
```

Feeding the above five lines into `jsnap` yields an encoding of the triangulation in SnapPea's file format; this was the input given to SnapPea in Example 4.1.

ACKNOWLEDGEMENTS

We would like to thank Mladen Bestvina and John Stallings for many helpful discussions, as well as Jeff Weeks and Bill Floyd for explaining SnapPea's intricacies. We would also like to express our gratitude to Kai-Uwe Bux for critiquing an early version of this paper.

ELECTRONIC AVAILABILITY

The software described here (binary and source files, complete online documentation and user manual) is available at http://www.math.uiuc.edu/~brinkman/.

REFERENCES

[A'Campo 1998] N. A'Campo, "Planar trees, slalom curves and hyperbolic knots", *Inst. Hautes Études Sci. Publ. Math.* **88** (1998), 171–180.

[Bestvina and Handel 1992] M. Bestvina and M. Handel, "Train tracks and automorphisms of free groups", *Ann. of Math.* (2) **135**:1 (1992), 1–51.

[Brinkmann 2000] P. Brinkmann, "An implementation of the Bestvina–Handel algorithm for surface homeomorphisms", *Experiment. Math.* **9**:2 (2000), 235–240.

[Burde and Zieschang 1985] G. Burde and H. Zieschang, *Knots*, de Gruyter, Berlin, 1985.

[Hemion 1979] G. Hemion, "On the classification of homeomorphisms of 2-manifolds and the classification of 3-manifolds", *Acta Math.* **142**:1-2 (1979), 123–155.

[Johannson 1979] K. Johannson, *Homotopy equivalences of 3-manifolds with boundaries*, Springer, Berlin, 1979.

[Lickorish 1964] W. B. R. Lickorish, "A finite set of generators for the homeotopy group of a 2-manifold", *Proc. Cambridge Philos. Soc.* **60** (1964), 769–778.

[Lyndon and Schupp 1977] R. C. Lyndon and P. E. Schupp, *Combinatorial group theory*, Ergebnisse der Math. **89**, Springer, Berlin, 1977.

[Mosher 1986] L. Mosher, "The classification of pseudo-Anosovs", pp. 13–75 in *Low-dimensional topology and Kleinian groups* (Coventry/Durham, 1984), edited by D. B. A. Epstein, London Math. Soc. Lecture Notes Series **112**, Cambridge Univ. Press, Cambridge, 1986.

[Stallings 1983] J. R. Stallings, "Topology of finite graphs", *Invent. Math.* **71**:3 (1983), 551–565.

[Thurston 1986a] W. P. Thurston, "Hyperbolic structures on 3-manifolds, II: Surface groups and 3-manifolds which fiber over the circle", preprint, 1986. See http://www.arxiv.org/abs/math.GT/9801045.

[Thurston 1986b] W. P. Thurston, *A norm for the homology of 3-manifolds*, Mem. Amer. Math. Soc. **339**, Amer. Math. Soc., Providence, RI, 1986.

[Thurston 1997] W. P. Thurston, *Three-dimensional geometry and topology*, vol. 1, Princeton Univ. Press, Princeton, NJ, 1997.

[Waldhausen 1968] F. Waldhausen, "On irreducible 3-manifolds which are sufficiently large", *Ann. of Math.* (2) **87** (1968), 56–88.

[Weeks 1993] J. R. Weeks, "SnapPea", software, 1993. Available at http://www.northnet.org/weeks/index/SnapPea.html.

Peter Brinkmann, Department of Mathematics, 273 Altgeld Hall, 1409 W. Green Street, Urbana, IL 61801, United States (brinkman@math.uiuc.edu)

Saul Schleimer, Department of Mathematics, 851 S. Morgan Street (MC 249), University of Illinois at Chicago, Chicago, IL 60607, United States (saul@math.berkeley.edu)

Received December 5, 2000; accepted in revised form April 5, 2001